Research article

Modeling nutrient removal and energy consumption in an advanced activated sludge system under uncertainty

Bartosz Szeląg [a,*], Adam Kiczko [b], Ewa Zaborowska [c], Giorgio Mannina [d], Jacek Mąkinia [c]

[a] *Department of Geotechnics and Water Engineering, Kielce University of Technology, Al. Tysiąclecia Państwa Polskiego 7, 25-314, Kielce, Poland*
[b] *Department of Hydraulic and Sanitary Engineering, Warsaw University of Life Sciences-SGGW (WULS), Nowowiejska 7, 02-797, Warsaw, Poland*
[c] *Department of Sanitary Engineering, Gdańsk University of Technology, Narutowicza Street 11/12, 80-233, Gdańsk, Poland*
[d] *Engineering Department, Palermo University, Viale delle Scienze, Ed.8, 90128, Palermo, Italy*

A B S T R A C T

Activated sludge models are widely used to simulate, optimize and control performance of wastewater treatment plants (WWTP). For simulation of nutrient removal and energy consumption, kinetic parameters would need to be estimated, which requires an extensive measurement campaign. In this study, a novel methodology is proposed for modeling the performance and energy consumption of a biological nutrient removal activated sludge system under sensitivity and uncertainty. The actual data from the wastewater treatment plant in Slupsk (northern Poland) were used for the analysis. Global sensitivity analysis methods accounting for interactions between kinetic parameters were compared with the local sensitivity approach. An extensive procedure for estimation of kinetic parameters allowed to reduce the computational effort in the uncertainty analysis and improve the reliability of the computational results. Due to high costs of measurement campaigns for model calibration, a modification of the Generalized Likelihood Uncertainty method was applied considering the location of measurement points. The inclusion of nutrient measurements in the aerobic compartment in the uncertainty analysis resulted in percentages of ammonium, nitrate, ortho-phosphate measurements of 81%, 90%, 78%, respectively, in the 95% confidence interval. The additional inclusion of measurements in the anaerobic compartment resulted in an increase in the percentage of ortho-phosphate measurements in the aerobic compartment by 5% in the confidence interval.

The developed procedure reduces computational and measurement efforts, while maintaining a high compatibility of the observed data and model predictions. This enables to implement activated sludge models also for the facilities with a limited availability of data.

1. Introduction

The International Water Association (IWA) Activated Sludge Models (ASMs) (Henze et al., 2000) have widely been accepted as a simulation tool in full-scale wastewater treatment plants (WWTPs). Those models have been used for either enhancing process understanding (Boiocchi et al., 2017), development of control strategies (e.g. Huang et al., 2020; Pocquet et al., 2016; Zaborowska et al., 2019), or diagnosis and optimization (Flores-Alsina et al., 2014; Mannina et al., 2011a,b; Mąkinia and Zaborowska, 2020; Wu et al., 2016). In terms of the cost optimization, aeration systems are the most significant energy consumers (up to 60%) in WWTPs (Gu et al., 2017; Henriques and Catarino, 2017). However, practical studies, specifically focused on the energy

consumption for aeration, have been published less frequently, primarily due to the lack of appropriate experimental data for model calibration and validation (e.g. Zaborowska et al., 2017; Zhao et al., 2019).

In order to use the ASMs for analyzing performance of WWTPs, a number of kinetic parameters should be adjusted (Fall et al., 2011; Henze et al., 2000; Zhu et al., 2015). Considering the number of identified parameters and interactions between them, the ASM calibration protocols have been expanded with sensitivity and uncertainty analysis (Mannina et al., 2011a,b). Sensitivity analysis, either local or global, is performed before the calibration stage to (1) identify the parameters that have a significant influence on model predictions, and (2) reduce the number of parameters to be adjusted at the calibration stage

---

([Mannina et al., 2011a,b](); [Sin et al., 2011]()). Despite the reduced number of parameters, their identification may be difficult due to potential strong interactions between the parameters ([Mannina et al., 2011a,b](), [2016](); [Sathyamoorthy et al., 2014](); [Zonta et al., 2014]()).

The local sensitivity analysis (LSA) methods, even though still useful for model calibration ([Cosenza et al., 2013]()), evaluate only local effects on the model outputs under small changes of a single parameter. In contrast, global sensitivity analysis (GSA) methods examine the effects of combinations of different parameters over a wide range of parameter values. Furthermore, uncertainty analysis is combined with GSA to determine the reliability of identified parameters and their effect on model outputs ([Belia et al., 2021](); [Lindblom et al., 2020]()). Due to the high computational demands in the GSA methods, simulation runs should rather be minimized.

In the WWTP calibration protocol of [Mannina et al. (2011a,b)](), uncertainty analysis allowed to establish the scatter of computational results in terms of the 95% confidence interval and reliability of the identified parameters. However, that protocol focused on the identification of model parameters for simulation of wastewater quality, while neglecting the energy-related aspects. Moreover, an appropriate selection of sampling points (their number and location) for model calibration was not considered in terms of the results of uncertainty analysis. It should be emphasized that a higher number of the sampling points reduces the uncertainty of model predictions, but the cost of measurement campaigns is increased.

This study presents a new methodology for modelling ASMs considering both nutrient compounds (NUC - S_{NH4-N}, S_{NO3-N}, S_{PO4-P}) and energy consumption for aeration with the uncertainty of kinetic parameters. A practical application of the developed methodology is shown for a large advanced WWTP. The multivariate adaptive regression spline (MARS) method was used to account for a variability in the assumed ranges of parameters during sensitivity analysis. In comparison with the multivariate linear regression method, the MARS is advantageous when dealing with non-linear relationships. Furthermore, the proposed methodology presents a novel solution based on the Generalized Likelihood Uncertainty Estimation (GLUE) analysis to (1) determine the variation ranges of model parameters, and (2) reduce computational demands in uncertainty analysis. With this approach, different combinations of the sampling points and measurement data could be for identification and distribution of parameters in the ASMs. This is an important advantage compared to the currently used methods, because the optimal selection of sampling points and the scope of measurements can be determined.

2. Material and methods

2.1. Study site

The studied plant is a large biological nutrient removal (BNR) facility treating municipal wastewater originating from the city of Słupsk (northern Poland) and surrounding communities. During the studied period, comprising the summer months, the average flow rate and pollutant load were approximately 22,000 m³/d and 190,000 PE (population equivalents), respectively. The effluent standards for the plant were established in accordance with the requirements of the EU Urban Wastewater Directive (91/21/EEC), i.e., the average annual total nitrogen (TN) and total phosphorus (TP) concentrations of 10 mg N/L and 1 mg P/L, respectively.

The biological step of the plant consists of three parallel trains with the bioreactors designed according to the A_2O process configuration ([Fig. 1]()). The total volume of one bioreactor is 10,000 m³ and the shares of the anaerobic (AN), anoxic (AO) and aerobic (AE) compartments are 14%, 29% and 57%, respectively.

The mixed liquor recirculation is directed from the end of the AE compartment to the first AO compartment, while the returned activated sludge (RAS) is recirculated to the head of the bioreactor. More details on the studied WWTP layout and performance can be found elsewhere ([Zaborowska et al., 2017](), [2019]()).

2.2. Methodology for modelling bioreactor performance and energy consumption under uncertainty

In the present study, the model developed by [Zaborowska et al. (2017)]() is subjected to a novel modelling procedure. This study explores a new approach to sensitivity analysis (GSA vs. LSA) and applies uncertainty analysis (GLUE method) while predicting an extended range of model outputs, i.e., NUC and E_{AIR}. The complete modelling procedure is shown in [Fig. 2](), highlighting the steps in the present study. In comparison with the methodology of Flores – [Avilés et al. (2019)](), [Mannina et al. (2011a,b)](), [Borzooei et al. (2019a](), [2019b)](), the following three new elements have been incorporated:

- Energy consumption for aeration is considered as a model output,
- Ranges of the variability of kinetic parameters are narrowed in uncertainty analysis,
- The number and location of sampling points are considered in uncertainty analysis.

2.2.1. Simulation tool

GPS-X ver 7.0 (Hydromantis, Canada) was used as a simulator environment with special utilities for the influent characterization and sensitivity analysis (see: Section 2.2.6).

2.2.2. Data collection (step 1)

The model has previously been calibrated based on laboratory experiments (batch tests under anaerobic/aerobic and anaerobic/anoxic conditions) and validated based on full-scale measurements (96-h campaigns in summer and winter) ([Zaborowska et al., 2017]()). In the present study, a new set of data was used from another 96-h measurement campaign. The bioreactor influent and effluent characteristics are shown in the Supporting Information (SI) ([Table S1]()). Grab samples were
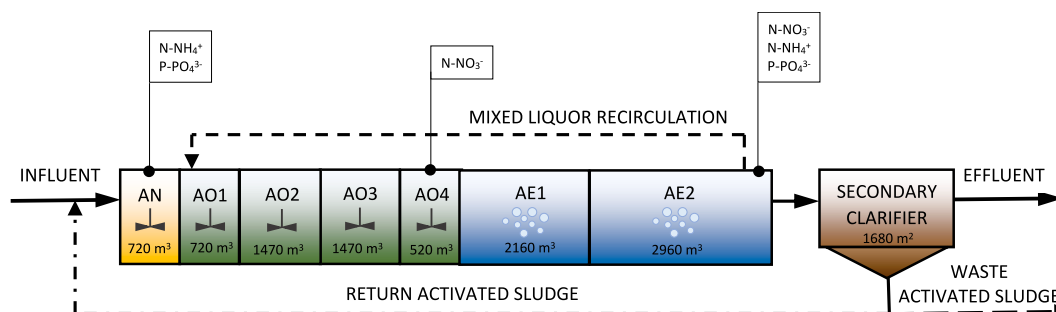

Fig. 1. Schematic layout of the bioreactor in the studied WWTP with the location of sampling points used as NUC (AN – anaerobic, AO – anoxic, AE – aerobic).
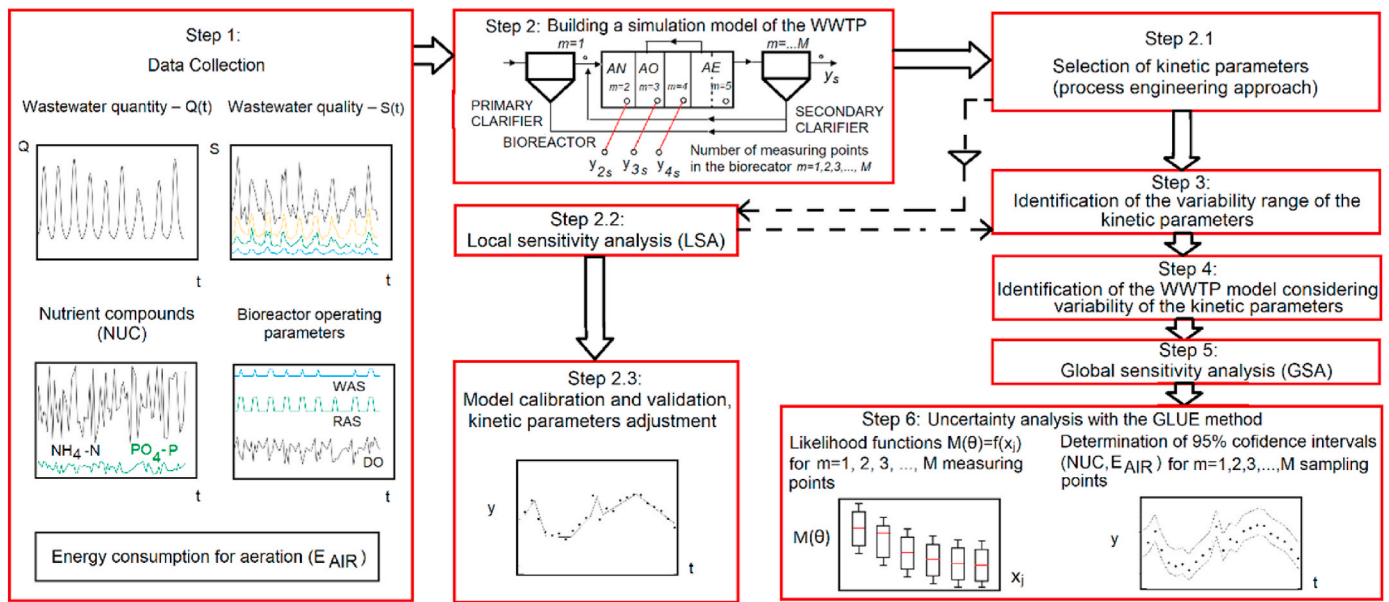
Fig. 2. Complete modelling procedure for the bioreactor (only steps 3–6 are considered in the present study).

withdrawn every 2 h at the following locations: inlet to the bioreactor, and outlets from the AN, AO and AE compartments. The samples were analyzed for several parameters, including total and volatile solids concentrations, chemical oxygen demand (COD) fractions as well as different nitrogen and phosphorus compounds. The detailed description of the measurement campaign can be found in Zaborowska et al. (2019). Concentrations of ammonium (NH_4^+-N) (S_{NH4}), nitrate (NO_3^--N) (S_{NO3}) and phosphate (PO_4^{3-}-P) (S_{PO4}) in the bioreactor were used in this study as the NUCs for sensitivity and uncertainty analysis. The blowers power supply (E_{AIR}) was recorded (in kWh) every 1 h by electricity meters.

2.2.3. Building a simulation model of the WWTP (step 2)

A simulation model of the studied WWTP was developed using the Activated Sludge Model No. 2 d (ASM2d) as a core model for biochemical processes (Henze et al., 2000). For the same model, applied in other WWTPs located in the northern Poland, the kinetic parameters were estimated using the Nelder-Mead simplex method with the maximum likelihood objective function (Mąkinia et al., 2006; Swinarski et al., 2012). In the study of Zaborowska et al. (2017), those kinetic parameters were adopted for the Slupsk WWTP with minor changes. The

accuracy of model predictions was confirmed by the coefficient of determination (R^2). In the calibration phase (laboratory experiments), the model predictions and measurements were strongly correlated (R^2 = 0.88–0.99). In a validation phase (full-scale experiments), a strong correlation was also obtained (R^2 = 0.54–0.72). The hydraulic model of the bioreactor was set as a series of completely stirred tank reactors ("tanks-in-series" model), including one anaerobic (AN), four anoxic (AO), and two aerobic (AE) tanks. The secondary clarifier was represented by a one-dimensional, non-reactive model by Takács et al. (1991). The influent characterization model (COD-based fractions) was developed in the Influent Advisor module incorporated in GPS-X.

2.2.4. Identification of the variability range of the kinetic parameters (step 3)

A review of literature data shows that the physically interpretable ranges of the kinetic parameters in the ASM2d can be very broad (e.g., Mąkinia and Zaborowska, 2020). Estimation of the variability ranges of kinetic parameters is a crucial step in uncertainty analysis. Thus, the present study implements a simple method of narrowing the variability ranges of kinetic parameters using the available measurement data
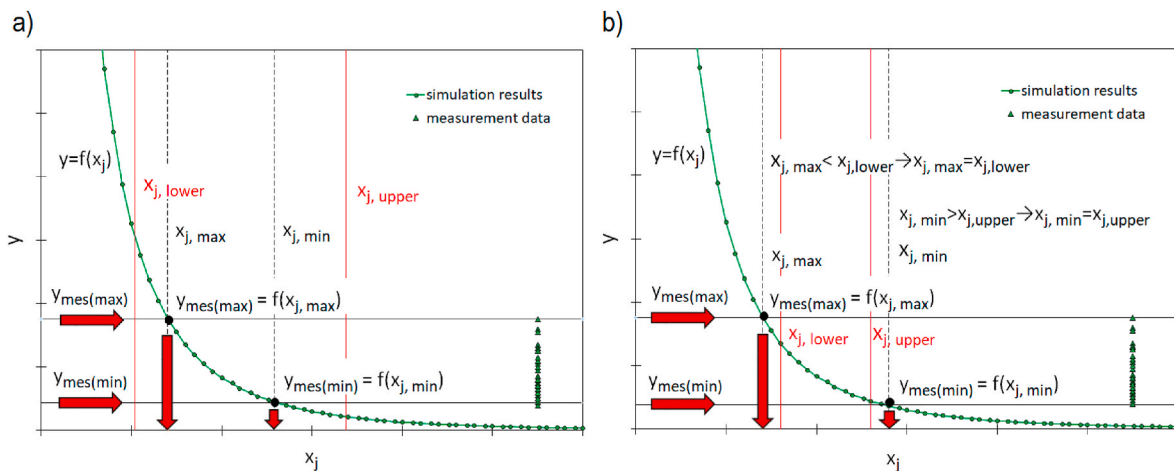

Fig. 3. Methodology for selecting the range of kinetic parameters (x_j) for uncertainty analysis when (a) the limits $x_{j,min}$ and $x_{j,max}$ determined from y = f(x_j) are within the typical range of variation ($x_{j,lower} \div x_{j,upper}$) of parameter **j**, and (b) the limits $x_{j,min}$ and $x_{j,max}$ determined from y = f(x_j) exceed the typical range of variation of parameter **j**.

(Fig. 3). Assuming that the value of parameter **j** changed in the range Δx_j, the variability of the measured output variables (NUC, E_{AIR}) was determined as follows: $y = f(x_1, x_2, x_j + i \cdot \Delta x_j, \ldots, x_k)$, where **i** is the calculation step.

For the maximum and minimum values of the measured output variables ($y_{mes(max)}$, $y_{mes(min)}$), the values of parameter **j** were determined as follows: $x_{j,max} = f(y_{mes(max)}, x_1, x_2, x_j, \ldots, x_k)$ and $x_{j,min} = f(y_{mes(min)} x_1, x_2, x_j, \ldots, x_k)$ (Fig. 3a). In a special case, when the determined values of $x_{j,min}$, $x_{j,max}$ exceeded the typical limits ($x_{j,lower}$, $x_{j,upper}$), the literature range would be preferred for uncertainty analysis (Fig. 3b).

2.2.5. Identification of the WWTP model considering the variability of kinetic parameters (step 4)

The Monte Carlo (MC) method was used to simulate the uncertainty of the calibrated kinetic coefficients from the assumed theoretical distributions. It was also assumed that the identified kinetic coefficients are independent, which enables to estimate their values from single distributions. Due to the probabilistic distribution of the identified model parameters, there is a required number of simulations in order to maintain the consistency of the assumed distributions. Using the MC method in this study, values of 10 kinetic coefficients were adjusted. In the previous study (Zaborowska et al., 2017), those coefficients were adjusted based on the process engineering approach. Considering the uncertainty of kinetic parameters, i.e., the fixed ranges determined in Section 2.3.4, MC simulations were run using a special GPS-X utility called "Monte Carlo Analyzer". The MC method is based on the distributions of the examined parameters and number of simulations (samples) for a series of independent tests. It was assumed in the present study that the distribution of the kinetic parameters was uniform. The number of samples was 5000, which fits in the reported range of 1000–10000 for WWTP simulation studies (Freni et al., 2009; Sin et al., 2011).

2.2.6. Global sensitivity analysis (step 5)

Considering non-linear relationships between the kinetic parameters and model outputs (NUC and E_{AIR}), a non-linear Multivariate Adaptive Regression Spline (MARS) model was proposed for GSA. This model has been used to simulate processes in the bioreactor (Wang et al., 2019), but it has not been used for GSA of a WWTP model yet. The MARS model describes the following general relationship:

$$y^* = \beta_0 + \sum_{j=1}^{M} \cdot h\left(x_j^*, t_j^*\right) \tag{1}$$

where: β_0, β_j– estimated empirical coefficients of the model by recursive partitioning of the feature space (Friedman and Roosen, 1995); M – number of the base functions $h(x_j^*, t_j^*)$; x_j^*- standardized values of the identified kinetic parameters, expressed as:

$$x_j^* = \frac{x_j - min\{x_j\}}{max\{x_j\} - min\{x_j\}} \quad x_j^* \in [0; 1] \tag{2}$$

y^*- standardized values of the NUC (S_{NH4-N}^*, S_{NO3-N}^*, S_{PO4-P}^*) and E_{AIR}^* expressed as:

$$y^* = \frac{y - min\{y\}}{max\{y\} - min\{y\}} \quad y^* \in [0; 1] \tag{3}$$

y – predicted value are determined as $\frac{\sum_{k=1}^{p} y_k(t)}{k}$ (where: k - number of the predicted values; j - specific NUC, E_{AIR} calculated in the four-day period; p - number of the time intervals). The base function $h(x_j^*, t_j^*)$ is defined as follows:

$$h\left(x_j^*, t_j^*\right) = \begin{cases} \beta_j \cdot \left(x_j^* - t_j\right) \, for \, x_j^* > t_j^* \\ 0 \, for \, x_j^* \le t_j^* \end{cases} \tag{4}$$

where: t_j^* – threshold values for M - base functions (Fig. S1); x_j^* – independent variables (kinetic parameters). For a compact description in MARS, Equation (4) is written as $\beta_j \cdot max(0, x_j^* - t_j^*)$.

Equation (1) is given in the form of a linear regression with the nodes with threshold values, t_j. Therefore, in the intervals of variation x_j^*, β_i can be identified with the sensitivity of a model. The sensitivity can be derived based on the slope angle (value β_j) between the abscissa and ordinate axes (Wang et al., 2019). The GSA with the MARS model requires consideration of the number of nodes for the subsequent independent variables and β_j variation. When two threshold values are determined for a single variable x_j^*, such that $t_1^* < t_2^*$ and $y = \beta_1 \cdot x_j^* + \ldots + \beta_0 \, (x_j^* > t_1^*)$ and $y = \beta_2 \cdot x_j^* + \ldots + \beta_0 \, (x_j^* > t_2^*)$, then the slope in the interval $[t_1^*; t_2^*]$ is $\beta_1 + \beta_2$. Assuming the number of nodes in the MARS model to be 0 for x_j, a multi-linear regression model (MLR) was developed. That model has frequently been used for GSA for WWTPs (Shahsavania et al., 2010). The values of β_j were used as a basis for the assessment of the influence of kinetic parameters on the predicted NUCs and E_{AIR}. For $\beta_j > 0.1$, the variable (β_j) was assumed to have a high influence on y (Cosenza et al., 2013). For the MARS model, such data are missing because they have not been used for sensitivity analysis. In the present study, the program STATISTICA 10 was used to determine the number of nodes, threshold values (t_j^*), and β_j coefficients in Equation (1). Statistically significant kinetic parameters were found automatically.

In order to compare the GSA calculations with Equation (1), simulations were also performed for the same range of kinetic parameters using MLR and dynamic LSA in the GPS-X "Sensitivity Analysis" module. The effect of the kinetic parameters was determined by calculating sensitivity coefficients (S_{ij}) for the variability in NUC (S_{NH4-N}, S_{NO3-N}, S_{PO4-P}) and E_{AIR} (Petersen et al., 2002).

2.2.7. Uncertainty analysis with the GLUE method (step 6)

The aim of uncertainty analysis was to assess interactions between kinetic parameters and identify their empirical distributions, for which good fits of measurements and simulations were obtained. The kinetic parameters considered in the analysis represent complex biochemical processes in the bioreactor (nitrification, denitrification, enhanced biological phosphorus removal (EBPR). This generates a large number of kinetic parameters for identification with a limited number of measurements (Fall et al., 2011). Although the kinetic parameters are correlated, this fact is neglected for uncertainty calculations in the GLUE method (Beven and Binley, 1992). Considering a correlation between the adjusted parameters, regression relationships between those parameters would be required (Chen and Han, 2021).

Uncertainty analysis of the model predictions was performed with the probabilistic GLUE method. In contrast to the deterministic approach with a single set of parameters, the distribution of parameters is estimated by the GLUE based on the Bayes formula (Beven and Binley, 1992):

$$M(\Theta / S) = \frac{M(S/\Theta) \cdot M(\Theta)}{\int M(S/\Theta) \cdot M(\Theta) dM(S/\Theta) d\Theta} \tag{5}$$

where $M(\Theta)$ is the a priori distribution of parameters; $M(S/\Theta)$ is the likelihood function, and $M(\Theta/S)$ is a posteriori distribution resulting from identification of parameters.

In practice, the assumption concerning a priori distribution is weak and takes the form of a uniform distribution. Thus, the selection of a likelihood function is crucial as the assumption of a priori uniform distribution may not be appropriate. With the likelihood function given in Equation (5), it was assumed that the model errors were uncorrelated and normally distributed. The variance of the model errors is $\kappa \cdot \sigma^2$. The following function was used for these analyses (Romanowicz and Beven, 2006):

$$M(c/\Theta) = exp\left[\frac{-\sum_{k=1}^{N}(S_k - \widehat{S_k})^2}{\kappa \cdot \sigma^2}\right] \tag{6}$$

where: κ – is the scaling parameter to control posteriori distribution variance, σ^2 – is the residual variance of the model, S_k, $\widehat{S_k}$ - are the measured data and predictions of the selected NUC and E_{AIR} in the subsequent and k-th time steps.

Using the measurement data (S_k) and model predictions ($\widehat{S_k}$) of the NUCs (S_{NH4-N}, S_{NO3-N}, S_{PO4-P}) and E_{AIR}, the value of κ was determined by minimizing the variance (measurements - model predictions) and maximizing the number of data points within the 95% confidence interval. The likelihood functions and multidimensional distribution of the kinetic parameters (a posteriori) were determined for the measurement data within the 95% confidence interval. Then, 95% confidence intervals were determined for the NUCs, i.e. S_{NH4-N}, S_{NO3-N}, S_{PO4-P}. In each case, the median values of the NUC and E_{AIR} were also determined.

In the present study, the GLUE analysis considered four scenarios of the measured data sets for model calibration and uncertainty analysis (Table S2). In Set 1, it was assumed that only the NUC data in the AE compartment were the basis for uncertainty analysis and model calibration. In Sets 2 and 3, specific measurements (S_{NH4-N} or S_{PO4-P}) in the AN compartment were added, whereas in Set 4, S_{NH4-N}, S_{NO3-N}, S_{PO4-P} in both AE and AN compartments were incorporated.

3. Results

3.1. Identification of the variability range of the kinetic parameters

The ranges of ten kinetic parameters, assumed for the GLUE uncertainty calculations, were determined using the GPS-X software and measurement data ($S_{NH4-N(AE, AN)}$, $S_{NO3-N(AE)}$, $S_{PO4-P(AE, AN)}$). The results were compared with the literature data and ASM2d default values (Table 1). In comparison with the literature data, the revised ranges of variation were narrowed for most of the considered kinetic parameters (μ_A, b_A, μ_H, K_{OH}, K_{OA}, q_{PHA}, q_{PP}, b_{PAO}).

3.2. Sensitivity analysis

3.2.1. Local sensitivity analysis

The LSA was performed in GPS-X for the set of 10 kinetic parameters adjusted in a previous study (Zaborowska et al., 2017). The values of sensitivity coefficients (S_{ij}) are shown in Table S3 in the SI. The kinetic parameters were ranked based on the effect on S_{NH4-N} (AN and AE compartments), S_{NO3-N} (AE compartment), S_{PO4-P} (AN and AE compartments). The calculations of LSA showed that μ_A, b_A, and $K_{NH,A}$ had the strongest influence on $S_{NH4-N(AE)}$ and those parameters were classified as extremely influential.

Among the other analyzed kinetic parameters, K_{OH} had a significant influence on $S_{NH4-N(AE)}$, whereas K_{OH} and b_A had the greatest (but insignificant) influence on the S_{NO3-N}. The q_{PHA} and q_{PP} were very influential on S_{PO4-P} concentrations in the AN and AE compartments, respectively, whereas b_{PAO} was influential in both compartments. The E_{AIR} was insignificantly influenced by all the analyzed kinetic parameters ($S_{ij} \leq 0.05$).

3.2.2. Global sensitivity analysis

Multiple linear regression. Using MC simulation results for the specific kinetic parameters (Table 1) and NUC in the AE and AN compartments, and $E_{AIR}*$ in the AE compartment, the β_j coefficients were determined by the MLR (Table 2).

In the AE compartment, b_A*, $K_{OH}*$, $q_{PP}*$ and k_h* had a strong effect ($\beta_j > 0.1$) on $S_{NH4-N}*$, $S_{NO3-N}*$, $S_{PO4-P}*$ and $E_{AIR}*$, respectively. In the AN compartment, b_A* and $q_{PHA}*$ were the most influential parameters affecting $S_{NH4-N}*$ and $S_{PO4-P}*$, respectively. For most of the analyzed kinetic parameters, the results of GSA by the MLR confirmed the previous LSA results. The results of MLR and LSA calculations for the NUCs in both AE ($S_{NH4-N}*$, $S_{NO3-N}*$, $S_{PO4-P}*$) and AN ($S_{PO4-P}*$) compartments showed that the same kinetic parameters influenced the analyzed biochemical processes. On the contrary, the values of S_{ij} and β_j revealed a different significance for the NUCs and $E_{AIR}*$. In the LSA method, the S_{ij} value for $K_{OH}*$ indicated an insignificant influence on $S_{NO3-N(AE)}*$, whereas the calculated β_j by the MLR suggested a strong effect of $K_{OH}*$ on the output. The LSA revealed that the kinetic parameters b_A* and μ_A* were insignificantly influential on $S_{NH4-N(AN)}*$ (Table 2). For $E_{AIR}*$, the LSA indicated an insignificant effect of the considered kinetic parameters, while the results of MLR indicated a strong effect of k_h* and rather small effect of b_A*, $K_{OH}*$, and μ_H*.

Multivariate Adaptive Regression Spline (MARS). Considering the obtained goodness-of-fits (R^2) of MLR to the data from the MC simulations (Table 2), the modified MLR method was used for sensitivity analysis. The determined threshold values of t_j* and β_j for statistically significant independent variables in the MARS models are shown in the SI (Tables S3–S4). The relationships between the kinetic parameters and model outputs (NUCs and E_{AIR}) were found to be non-linear and confirmed by the high values of R^2. Based on the coefficients specified in Tables S4–S7 in the SI, a sample equation in the MARS method for simulating normalized $S_{NH4-N}*$ values is given as follows:

Table 1
Summary of the variability ranges of 10 kinetic parameters for analysis.

| Kinetic parameter	Symbol	Units	ASM2d default value	Value (calibration)	Range (literature[a, b])	Calculated range
Hydrolysis rate	k_h	d^{-1}	3	3	0.96–3.00	**0.96–3.00**
Autotrophic maximum specific growth rate	μ_A	d^{-1}	1	1.05	0.20–1.20	**0.80–1.20**
Autotrophic decay rate	b_A	d^{-1}	0.2	0.15	0.04–0.20	**0.05–0.20**
Oxygen half saturation coefficient for autotrophic growth	$K_{O,A}$	mgO_2/l	0.5	0.5	0.40–3.00	**0.4–1.20**
Ammonium half saturation coefficient for autotrophic growth	$K_{NH,A}$	mgN/l	1	1.2	0.50–1.50	**0.50–1.50**
Heterotrophic maximum specific growth rate	μ_H	d^{-1}	6	3	0.60–13.20	**2.10–6.00**
Oxygen half saturation coefficient for heterotrophic growth	$K_{O,H}$	mgO_2/l	0.2	0.08	0.10–1.00	**0.10–0.50**
Rate constant for storage PHA	q_{PHA}	d^{-1}	6	6	0.30–10.00[b]	**1.30–6.00**
Rate constant for storage of poly- P	q_{PP}	d^{-1}	1.5	4.5	0.00–8.00[a]	**0.80–4.50**
Poly - p accumulating biomass lysis rate	b_{PAO}	d^{-1}	0.2	0.2	0.10–0.25	**0.12–0.25**

[a] Zaborowska et al. (2019).
[b] The upper range from Mąkinia et al. (2006).

Table 2

β_j coefficients determined by the MLR for the NUCs and $E_{AIR}*$.

Variables	$S_{NH4-N(AE)}*$	$S_{NO3-N(AE)}*$	$S_{PO4-P(AE)}*$	$S_{NH4-N(AN)}*$	$S_{PO4-P(AN)}*$	$E_{AIR}*$
μ_H*	−0.0029	−0.0185	*0.0510*	0.0046	*−0.0696*	*0.0396*
$K_{OH}*$	0.0015	*−0.5000*	−0.0414	−0.0067	*0.0690*	*−0.0567*
μ_A*	*−0.0644*	0.0147	−0.0029	*−0.0640*	0.0091	0.0257
b_A*	*0.1120*	−0.0221	−0.0010	*0.1140*	−0.0213	*−0.0579*
$K_{OA}*$	*0.0430*	0.0121	−0.0030	*0.0430*	−0.0070	*−0.0128*
$K_{NH,A}*$	*0.0499*	*−0.0302*	0.0026	*0.0490*	−0.0122	0.0034
$q_{PHA}*$	0.0117	*0.0409*	*−0.1306*	−0.0150	*0.3040*	−0.0089
$q_{PP}*$	0.0021	−0.0062	*−0.1571*	−0.0096	0.0340	0.025
$b_{PAO}*$	−0.0053	−0.0186	*0.1180*	0.0096	*−0.1340*	0.0244
k_h*	*0.0057*	*−0.0952*	−0.0260	0.0007	*0.0520*	*0.3546*
Intercept	0.0380	0.8860	0.1720	0.0350	0.0630	0.588
	$R^2 = 0.52$	$R^2 = 0.94$	$R^2 = 0.44$	$R^2 = 0.55$	$R^2 = 0.90$	$R^2 = 0.63$

Where: italic bold black indicates the most influential kinetic parameters for the NUC and E_{AIR} calculations; bold black (shadowed cells) indicates statistically significant parameters in the MLR.
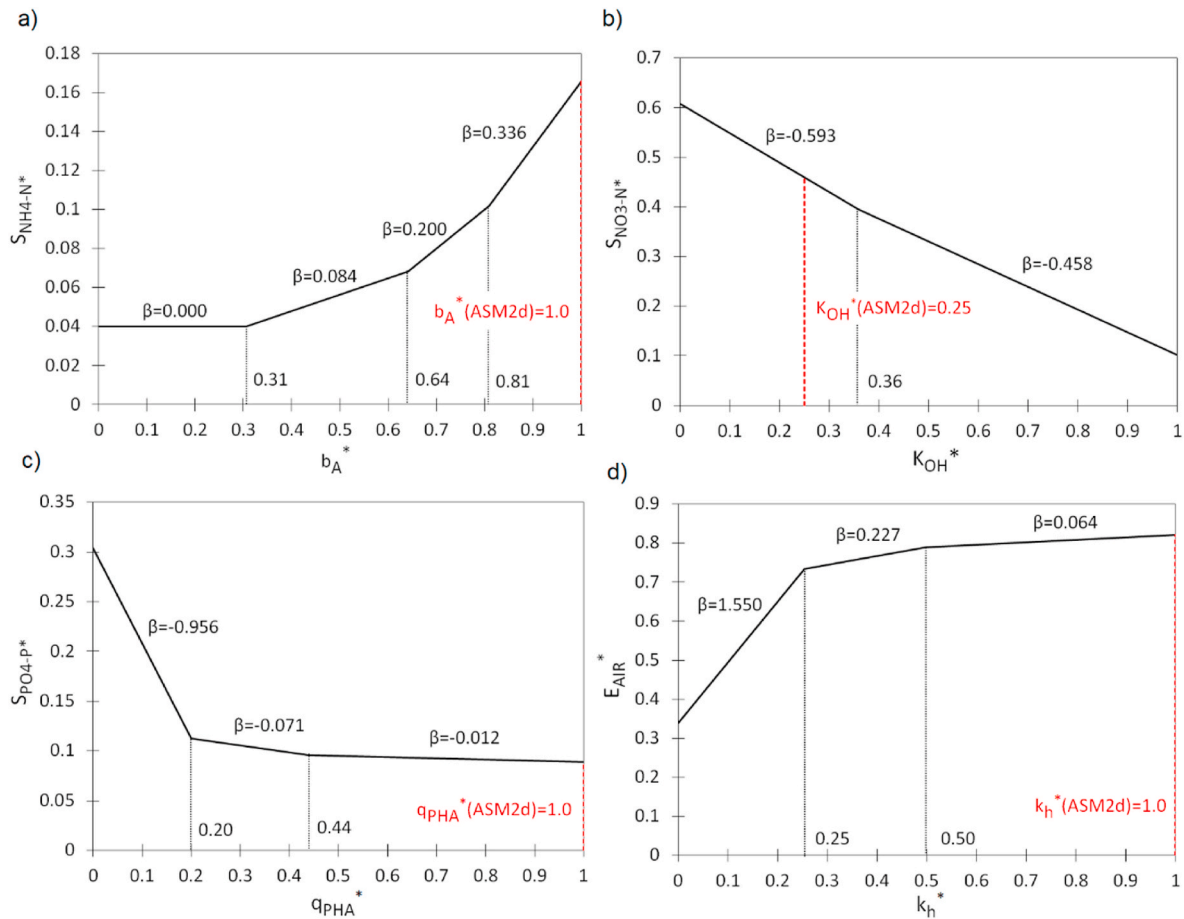
Fig. 4. Variability of the NUCs ($S_{NH4-N}*$, $S_{NO3-N}*$, $S_{PO4-P}*$), $E_{AIR}*$ and β_j in terms of the normalized kinetic parameters: a) b_A*, b) $K_{OH}*$, (c) $q_{PHA}*$, (d) k_h*.

$$S^*_{NH4-N(AE)} = 0.04 + 0.08 \cdot \max\left(0; b^*_A - 0.31\right) + 0.12 \cdot \max\left(0; b^*_A - 0.64\right) + 0.14 \cdot \max\left(0; b^*_A - 0.81\right)$$
$$-0.09 \cdot \max\left(0; \mu^*_A - 0.45\right) - 0.15 \cdot \max\left(0; 0.45 - \mu^*_A\right) + 0.07 \cdot \max\left(0; \mu^*_A - 0.21\right) + 0.06 \cdot \max\left(0; K^*_{NH} - 0.38\right)$$
$$-0.03 \cdot \max\left(0; 0.38 - K^*_{NH}\right) + 0.06 \cdot \max\left(0; K^*_{OA} - 0.51\right) - 0.03 \cdot \max\left(0; 0.51 - K^*_{OA}\right) - 0.01 \cdot \max\left(0; k^*_h - 0.86\right) - 0.01 \cdot \max\left(0; 0.99 - b^*_{PAO}\right)$$
$$+0.01 \cdot \max\left(0; q^*_{PP} - 0.16\right) + 0.01 \cdot \max\left(0; 0.16 - q^*_{PP}\right) \quad R^2 = 0.634 \tag{8}$$

In the MARS model, the R^2 values for $S_{NH4-N(AE)}^*$ were 22% higher than in the MLR. For $S_{NH4-N(AN)}^*$, $S_{PO4-P(AE)}^*$, and E_{AIR}^*, R^2 increased in the MARS model by 31%, 56%, and 46%, respectively, compared to the MLR. At least two threshold values were estimated with respect to the statistically significant kinetic parameters for the specific NUC, i.e., S_{NH4-N}^* - b_A^*, μ_A^*; S_{NO3-N}^*- K_{OH}^*; S_{PO4-P}^* - q_{PHA}^*, q_{PP}^*, b_{PAO}^*; E_{AIR}^* – k_h^* (Tables S4–S7 in the SI). The β_j values in the ranges of the normalized kinetic parameters showed a high variability, which indicated a variable sensitivity of the model in those ranges. In Fig. 4, the relationships $\beta_j = f(x_j^*)$ are shown for the NUCs* and E_{AIR}^* for the kinetic parameters with the highest values of S_{ij} and β_j. Tables S8–S11 in the SI contain the β values for the models to predict the NUC and E_{AIR} with respect to the analyzed kinetic parameters. For example, the relationship $S_{NH4-N}^* = f(b_A^*, \beta)$ can be described by three linear functions with the β_j values varying in the appropriate b_A^* ranges as shown in Fig. 4a. The obtained curves showed that β was increasing with the increasing b_A^*, which confirmed an increased model sensitivity. For the b_A^* range of 0–0.31, there was no influence of that parameter on S_{NH4-N}^* ($\beta = 0.00$). For the b_A^* range of 0.31–0.64, $\beta = 0.084$ which means that S_{NH4-N}^* increased from 0.040 to 0.068 in that range. For the b_{A*}^* range of 0.64–0.81, $\beta = 0.200$ and S_{NH4-N}^* increased from 0.068 to 0.102. The highest model sensitivities for S_{NO3-N}^* ($\beta = -0.593$) and S_{PO4-P}^* ($\beta = -0.956$) were obtained in the ranges of $K_{OH}^* = 0.0-0.36$ (Fig. 4b) and $q_{PHA}^* = 0.00-0.20$ (Fig. 4c), respectively.

The lowest value of $\beta = -0.012$ was obtained for the q_{PHA}^* range of 0.44–1.00. With respect to E_{AIR}^*, the highest model sensitivity ($\beta = 1.55$) was obtained for the k_h^* range of 0.00–0.25. For $k_h^* > 0.5$, the

influence of that parameter on E_{AIR}^* decreased approximately 25 times (Fig. 4d).

3.2.3. Uncertainty analysis with the GLUE method

For the assumed variation ranges of 10 kinetic parameters (Table 2), a series of MC simulations (5000 samples) were performed using the GPS-X "Monte Carlo Analyzer". Based on those simulation results, 95% confidence intervals of the variability of the NUC and E_{AIR} were determined for each calibration scenario (Sets 1–4 in Table S1 in the SI). Simulation results for all the analyzed calibration sets during the four-day measurement campaign can be found in the SI (Figs. S2–S7). Table S12 shows the percentage of the measured data in the calculated 95% confidence intervals. Figs. 5–6 show the 95% confidence intervals for the NUC and E_{AIR} in the scenario with the full set of measured data (Set 4). The highest proportion of measured data (NUC, E_{AIR}) within the 95% confidence interval was obtained for Sets 3 and 4 (Table S12). Sets 1 and 2 resulted in a smaller proportion of $S_{PO4-P(AE)}$ measurements in the calculated 95% confidence interval compared to Sets 3 and 4. In addition, Set 1 resulted in a smaller percentage of data in the 95% confidence interval for E_{AIR}. In comparison with Set 1, the incorporation of $S_{NH4-N(AN)}$ did not influence the 95% confidence interval and variability of the median NUC. The results for Sets 1 and 3 (Fig. S2b in the SI) indicated that the consideration of $S_{PO4-P(AN)}$ in model calibration resulted in a decreased $S_{NH4-N(AE)}$ median (calculation from the GLUE).

Moreover, the number of data points within the 95% confidence interval decreased for $S_{NH4-N(AE)}$, $S_{PO4-P(AE)}$ and $S_{PO4-P(AN)}$. On the contrary, an increased number of data points within the 95% confidence interval was identified for $S_{PO4-P(AN)}$ (Fig. S7d in the SI). It should also be noted that the difference in the absolute errors of model predictions

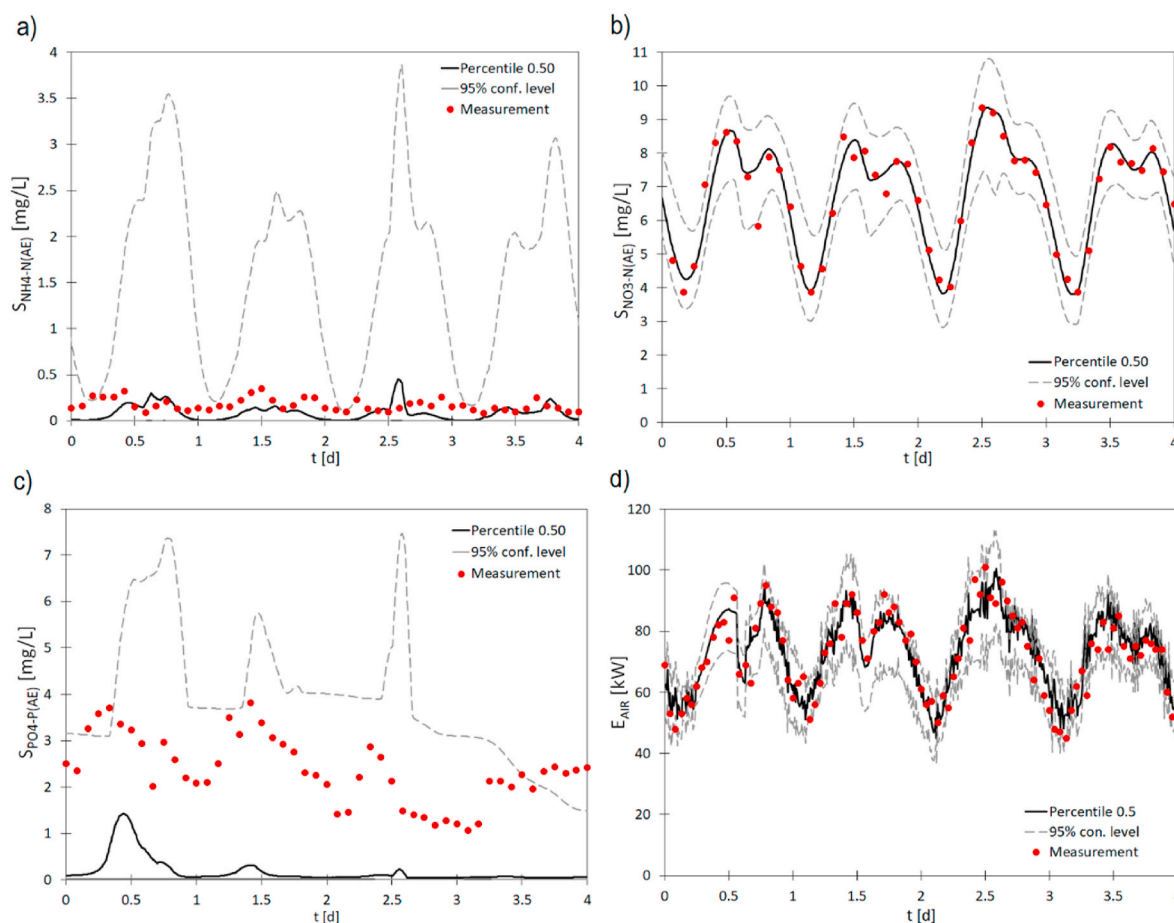**Fig. 5.** Comparison of the 95% confidence intervals in the AE compartment: a) $S_{NH4-N(AE)}$, b) $S_{NO3-N(AE)}$, c) $S_{PO4-P(AE)}$, d) E_{AIR} (solid line - median obtained by GLUE simulation; dashed line - lower and upper limits of the 95% confidence interval).
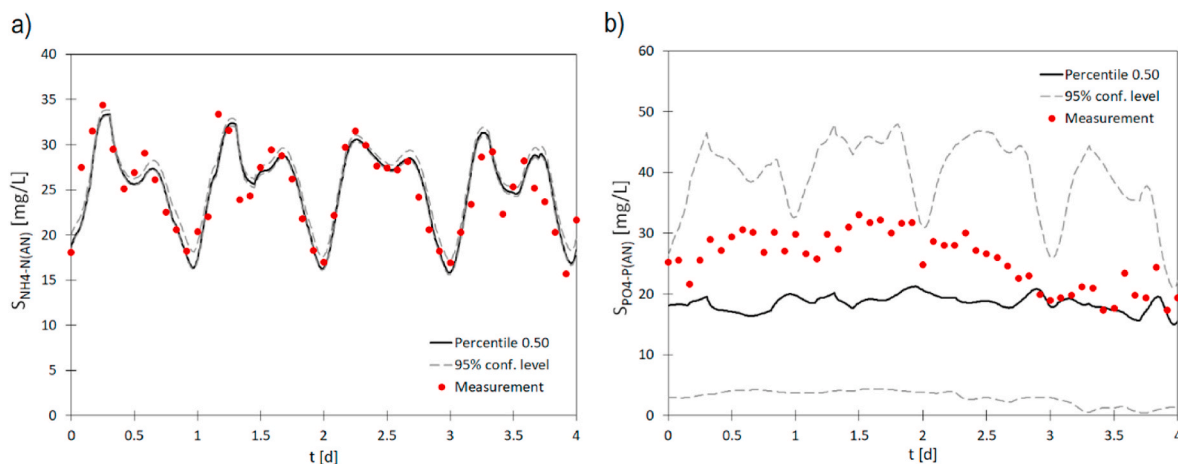
Fig. 6. Comparison of the 95% confidence intervals in the AN compartment: a) $S_{NH4-N(AN)}$, b) $S_{PO4-P(AN)}$ (solid line - median obtained by GLUE simulation; dashed line - lower and upper limits of the 95% confidence interval).
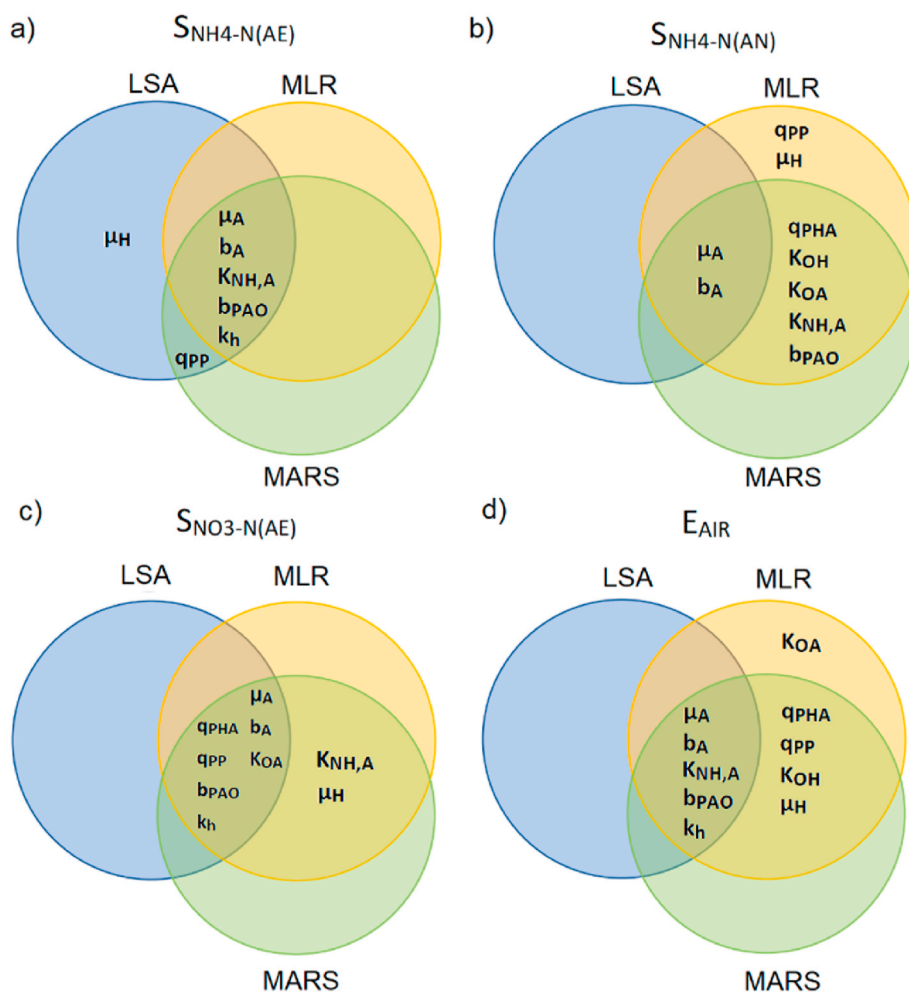

Fig. 7. Venn diagrams showing the results of LSA, MLR, MARS calculations for (a) $S_{NH4-N(AE)}$, (b) $S_{NH4-N(AN)}$, (c) $S_{NO3-N(AE)}$, (d) E_{AIR}.

decreased for the NUCs. In terms of the median from the GLUE, the largest difference was found for $S_{PO4-P(AN)}$, i.e., 10 mg P/L for Set 2 vs. 15 mg P/L for Sets 1, 3, 4. The results for S_{PO4-P} reflect a high uncertainty of model predictions. The results confirmed previous findings (Zaborowska et al., 2017; Hvala et al., 2018) that the behavior of phosphorus compounds is difficult to predict. Nevertheless, while applying the proposed methodology, the confidence intervals obtained

in this study were narrower compared with to Mannina et al. (2011a,b).

4. Discussion

4.1. Analysis of the results obtained by the LSA, MLR and MARS methods

The results for S_{PO4-P} are similar in all the applied sensitivity analysis

methods (Fig. S8 in the SI). For the analyzed NUCs (S_{NH4-N}, S_{NO3-N}) and E_{AIR}, the results obtained by the LSA and GSA methods (MLR, MARS) are different as shown by Venn diagrams in Fig. 7. The diagrams show similarities and differences between the results obtained by the three applied sensitivity analysis methods. The influence of kinetic parameters, in particular q_{PHA}, q_{PP}, b_{PAO}, on the behavior of S_{PO4-P} in both AE and AN compartments (Tables S8 and S11 in SI) has previously been confirmed by Mannina et al. (2011a,b). The results of sensitivity analysis by LSA, MLR, and MARS methods for $S_{NH4-N(AE)}$ are highly consistent (Fig. 7a). The influence of q_{PP} on $S_{NH4-N(AE)}$ was clearly shown using the MARS and LSA methods (but not MLR). These relationships were confirmed by Mąkinia et al. (2005) for a bioreactor operated in the Johannesburg process configuration (Table S13 in the SI). The results of Zaborowska et al. (2017) and Cosenza et al. (2013, 2014) also showed a strong influence of μ_A on $S_{NH4-N(AE)}$ predictions.

The results for $S_{NH4-N(AN)}$ are highly variable between the sensitivity analysis methods (Fig. 7b). The computational results showed the influence of μ_A and b_A on S_{NH4-N} in the AE compartment. This relationship was confirmed by Mannina et al. (2011a,b), Cosenza et al. (2013), (2014) and Zaborowska et al. (2019) (Table S13 in the SI). The MLR and MARS calculations showed the influence of q_{PHA}, K_{OH}, K_{OA}, $K_{NH,A}$, and b_{PAO} on the behavior of $S_{NH4-N(AN)}$.

Simulations by Mannina et al. (2011a,b) confirmed the influence of K_{OA}, $K_{NH,A}$ and b_{PAO} on the analyzed NUC in the AN compartment. The results of LSA, MLR, MARS methods for $S_{NO3-N(AE)}$ are highly correlated (Fig. 7c) and the simulation results (Fig. 7c) confirm the relationship $S_{NO3-N(AE)} = f(K_{OA})$ (Cosenza et al., 2013). Mąkinia et al. (2005) showed the influence of q_{PHA} and k_h on the predicted NUC ($S_{NH4-N(AE)}$, S_{PO4-P}). The results of the MLR and MARS methods showed the relationship $S_{NO3-N(AE)} = f(K_{NH,A}, \mu_H)$, which was also found by Cosenza et al. (2014). In addition to the wastewater quality aspects, the performed sensitivity analysis comprised E_{AIR} (Fig. 7d). The results of LSA, MLR, and MARS confirmed the influence of μ_A, b_A, $K_{NH,A}$, b_{PAO}, k_h on E_{AIR}. These results are consistent with the findings of Benedetti et al. (2012) for an A_2O bioreactor. The calculations performed with the MLR and MARS methods also showed the influence of q_{PHA}, q_{PP}, K_{OH}, and μ_H on predictions of E_{AIR}. It should be noted, however, that the significance of the kinetic parameters was only revealed in the GSA methods, while the LSA showed much lower influence on E_{AIR}. It was demonstrated that the method selected for sensitivity analysis could affect further steps in the modelling procedure and eventually model predictions. These findings are particularly important for designing the aeration system (Bischof et al., 1996, Flores-Alsina et al., 2012), energy assessment of the system operation, control and regulation (Åmand et al., 2013), and decision-making process in WWTPs (Borzooei et al., 2019a, 2019b;

2020a, 2020b).

Based on the performed analysis, the kinetic parameters were grouped under two main categories. The first group comprises the kinetic parameters (μ_A, b_A, and q_{PP}), which have a strong influence on the predicted NUC and E_{AIR} in a narrow range of their variation. The second group comprises the kinetic parameters, such as k_h, μ_H, K_{OH}, q_{PHA}, and b_{PAO}, which have a strong influence on the NUC and E_{AIR} values over a wide range of their variation.

4.2. The relationship between the sensitivity coefficient in LSA and the β_j coefficients in the MLR and MARS methods

Based on the results of LSA, MLR and MARS, a relationship between the S_{ij} and β_j coefficients, $S_{ij} = f(\beta_j)$, was developed for the NUC (S_{NH4-N}, S_{NO3-N}, S_{PO4-P} in the AE and AN compartments) and E_{AIR}. The relationship was described by a second-degree polynomial (Table S14 in the SI). The aim of the analysis was to investigate the nature of a relationship between the sensitivity coefficients obtained by the LSA, MARS and MLR. Specifically, the sensitivity was assessed in terms of the variability of kinetic parameters β_j (MARS), using the mean values of the S_{ij} calculated by the MLR method. It should be noted that the relationships between the S_{ij} and β_j, shown in Fig. 8 and Fig. 9, are not universal, but reflect the specific correlation between the sensitivity coefficients obtained by different methods. A similar approach can be found in (Cosenza et al., 2013). The best fit between the theoretical and empirical results was found for $S_{NH4-N(AN)}$ with $R^2 = 0.98$, while no linear relation $S_{ij} = f(\beta_j)$ was obtained for E_{AIR} (Fig. 8). The appropriate transformations $S_{ij} = f(\beta_j)$ can also be used to determine β_j in the MLR method.

In this study, the calculation of β_j in the MARS method was based on S_{ij} for the NUC and E_{AIR} (Figs. S9S–S12 in the SI) and the R^2 values were 0.54, 0.57, and 0.68 for $S_{NO3-N(AE)}$, $S_{PO4-P(AN)}$, and $S_{NH4-N(AE)}$, respectively (Fig. 9). This confirmed that the relationship $\beta_j = f(S_{ij})$ can be described by second- and third-degree polynomials (Table S15 in the SI). Fig. 9a and b shows sample curves for $S_{NO3-N(AE)}$ and E_{AIR} as the extreme cases for which the relationship $\beta_j = f(S_{xi})$ was found as indicated by the determined R^2 values. The data in Fig. 9a and b shows a decreasing trend of the correlation S_{ij} - β_j for the MARS model compared to the results of the MLR method. These differences are due to the fact that in the applied approach (MARS method), the sensitivity of the model considering the numerical values of kinetic parameters, changes rather locally in comparison with the results of LSA and MLR methods (Fig. 6). Therefore, a single kinetic parameter can have simultaneously a low and high influence on the calculation results (e.g., k_h in Fig. 9). In the LSA and MLR methods, single values of S_{ij} and β_j can correspond to several values of β_j in the MARS method. A strong model non-linearity can result in a decrease in the correlation $\beta_j = f(S_{ij})$, as shown for E_{AIR} and S_{NO3-N}. The results in Fig. 9b and Figs. S9–S12 show a decreasing trend in the correlation between β_j and S_{ij} for the MARS method compared to the MLR method. This means that the values of β_j in the MARS model can be determined from S_{ij} only in a limited range.

The novelty of the proposed approach relies on the application of sensitivity analysis for the ASMs in the appropriate ranges of kinetic parameters. In the existing methods (e.g., Cosenza et al., 2013), the model sensitivity is identified by a single coefficient over the full range of variation. On the contrary, the analysis performed in this study showed that the model sensitivity can actually be highly variable.

4.3. Advantages and disadvantages of the examined sensitivity analysis methods

With the approach proposed in this study, it is possible to identify the ranges of kinetic parameters of complex ASMs in which the NUC and E_{AIR} are influenced. The existing sensitivity analysis methods (Mannina et al., 2011a,b; Cosenza et al., 2014) neglect this aspect. The only information that can be obtained from those methods is whether a kinetic parameter influences the process under consideration. In comparison
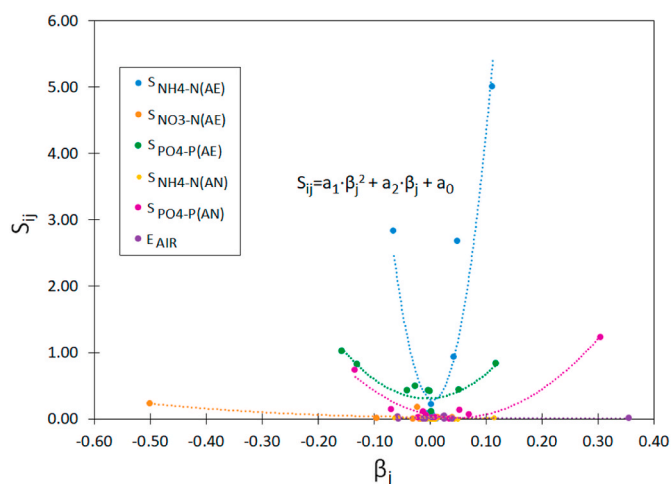

Fig. 8. The relationship $S_{ij} = f(\beta_j)$ for the NUC (S_{NH4-N}, S_{NO3-N}, S_{PO4-P}) in the AE and AN compartments, and E_{AIR}.

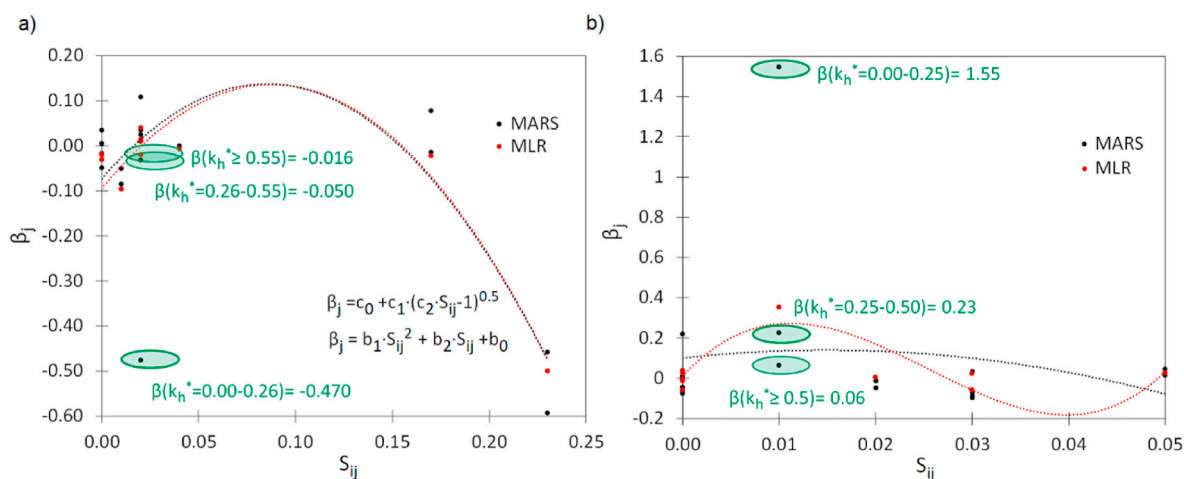**Fig. 9.** Relationship between the sensitivity coefficient (S_{ij}) and the coefficients β_j in the MLR and MARS model for (a) $S_{NO3-N(AE)}$, (b) E_{AIR}.

with the methods of Sin et al. (2011) and Mannina (2011a,b), the proposed approach is more advantageous because the variability of model sensitivity allows to better understand and estimate the influence of the kinetic parameters on model predictions. In the MARS model, sensitivity is considered in a wider range compared to LSA and MLR. The proposed method allows to identify cases, in which a specific kinetic parameter influences model predictions, while this influence becomes negligible in a wider range of its variation. This allows to determine such ranges of the variation of kinetic parameters, for which the optimal selection of parameters may be problematic. The narrowed ranges of the kinetic parameters may result in a reduced number of MC simulations. This acelerates the calculations of uncertainty analysis and improves predictions of the NUC and E_{AIR}.

The proposed method can establish such ranges of the variation of kinetic parameters, in which those parameters have a negligible influence on the model sensitivity (NUC and E_{AIR}). In such a case, the default values can be assumed and a range of the variability of kinetic parameters covered by MC simulations may be limited. As a consequence, the computational effort and execution time can be reduced in comparison with the existing sensitivity analysis methods (Mannina et al., 2011a,b; Saltelli et al., 2007; Sin et al., 2011), which are also based on MC simulations.

The currently available calibration protocols of ASMs, summarized by Mąkinia and Zaborowska (2020), neglect energy considerations. In this study, the results of sensitivity and uncertainty analyses examined the influence of several kinetic parameters on E_{AIR}, which is important for process control and optimization (Boroozei et al.,. 2020; Flores-Alsina et al., 2014). In contrast to LSA, the relevance of E_{AIR} was demonstrated in GSA while considering the interactions between the kinetic parameters. In particular, k_h was highly influential on E_{AIR}. This effect has not been reported in previous studies (Benedetti et al., 2012; Sin et al., 2008), which could be due to the available input data from laboratory experiments or full-scale measurements. On the other hand, E_{AIR} represents the total energy required for aeration and thus k_h relevance may result from the total amount of organic matter and organic nitrogen available for oxidation. Flores-Alsina et al. (2012) developed a non-linear relationship for Operational Cost Index (OCI) OCI = f(μ_A), but did not discuss the advisability of determining μ_A from operational data. In terms of the reliability of E_{AIR} predictions, it is advised to develop independent theoretical models to determine k_h in order to control the variability of that parameter. The GLUE method proposed in this study includes examination of the influence of a number of sampling points and their location (AN and AE compartments) on the identification of kinetic parameters. This approach allows for selection of the cost and time efficient scope of measurements ensuring that the model predictions

(NUC, E_{AIR}) remain within the acceptable confidence intervals.

5. Conclusions

A significant statistical significance of the kinetic parameters for E_{AIR} was found with GSA (but not with LSA) when considering the interactions between those parameters. Moreover, identification of the variability range of kinetic parameters is combined with GSA using the MARS method. With this approach, the variability range of kinetic parameters is narrowed, which reduces computational efforts and simulation time. In the GLUE method, the location of sampling points can be searched for a combination of measurement data to minimize the number of analyses without deteriorating the efficiency of model predictions. Moreover, identification of the variability range of kinetic parameters is combined with GSA using the MARS method. With this approach, the variability range of kinetic parameters is narrowed, which reduces computational efforts and simulation time. In the GLUE method, the location of sampling points can be searched for a combination of measurement data to minimize the number of analyses without deteriorating the efficiency of model predictions.

Declaration of competing interest

The authors declare the following financial interests/personal relationships which may be considered as potential competing interests: Bartosz Szelag reports was provided by Kielce University of Technology. Bartosz Szelag reports a relationship with Kielce University of Technology that includes: employment.

Data availability

Data will be made available on request.

Appendix A. Supplementary data

Supplementary data to this article can be found online at https://doi.

org/10.1016/j.jenvman.2022.116040.

References

Åmand, L., Olsson, G., Carlsson, B., 2013. Aeration control – a review. Water Sci. Technol. 67, 2374–2398. https://doi.org/10.2166/wst.2013.139.

Avilés, A.B.L., Velázquez, F.D.C., del Requelme, M.L.P., 2019. Methodology for energy optimization in wastewater treatment plants. Phase I: control of the best operating conditions. Sustainability 11, 1–18. https://doi.org/10.3390/su11143919.

Belia, E., Neumann, M.B., Benedetti, L., Johnson, B., Murthy, S., Stefan Weijers, S., Vanrolleghem, P.A., 2021. Uncertainty in Wastewater Treatment Design and Operation. IWA Publishing, London.

Benedetti, L., Batstone, D.J., De Baets, B., Nopens, I., Vanrolleghem, P.A., 2012. Uncertainty analysis of WWTP control strategies made feasible. Water Qual. Res. 47, 14–29. https://doi.org/10.2166/wqrjc.2012.038.

Beven, K., Binley, A., 1992. The future distributed models: model calibration and uncertainty prediction. Hydrol. Process. 6, 279–298. https://doi.org/10.1002/hyp.3360060305.

Bischof, F., Höfken, M., Durst, F., 1996. Design and construction of aeration systems for optimum operation of large wastewater treatment plants. Water Sci. Technol. 33, 189–198. https://doi.org/10.1016/0273-1223(96)00473-8.

Boiocchi, R., Gernaey, K.V., Sin, G., 2017. Understanding N2O formation mechanisms through sensitivity analyses using a plant-wide benchmark simulation model. Chem. Eng. J. 317, 935–951. https://doi.org/10.1016/j.cej.2017.02.091.

Borzooei, S., Amerlinck, Y., Abolfathi, S., Panepinto, D., Nopens, I., Lorenzi, E., Meucci, L., Zanetti, M.C., 2019a. Data scarcity in modelling and simulation of a large-scale WWTP: stop sign or a challenge. J. Water Proc. Eng. 28, 10–20. https://doi.org/10.1016/j.jwpe.2018.12.010.

Borzooei, S., Campo, G., Cerutti, A., Meucci, L., Panepinto, D., Ravina, M., Riggio, V., Ruffino, B., Scibilia, G., Zanetti, M., 2019b. Optimization of the wastewater treatment plant: from energy saving to environmental impact mitigation. Sci. Total Environ. 69, 1182–1189. https://doi.org/10.1016/j.scitotenv.2019.07.241.

Borzooei, S., Amerlinck, Y., Panepinto, D., Abolfathi, S., Nopens, I., Scibilia Meucci, G.L., Zanetti, M.C., 2020a. Energy optimization of a wastewater treatment plant based on energy audit data: small investment with high return. Environ. Sci. Pollut. Res. Int. 27, 17972–17985. https://doi.org/10.1007/s11356-020-08277-3.

Borzooei, S., Miranda, G.H.B., Abolfathi, S., Scibilia, G., Meucci, L., Zanetti, M.C., 2020b. Application of unsupervised learning and process simulation for energy optimization of a WWTP under various weather conditions. Water Sci. Technol. 81, 1541–1551. https://doi.org/10.2166/wst.2020.220.

Chen, Z., Han, S., 2021. Comparison of dimension reduction methods for DEA under big data via Monte Carlo simulation. Int. J Manag Sci Eng. 6, 363–376. https://doi.org/10.1016/j.jmse.2021.09.008.

Cosenza, A., Mannina, G., Vanrolleghem, P.A., Neumann, M.B., 2013. Global sensitivity analysis in wastewater applications: a comprehensive comparison of different methods. Environ. Model. Software 49, 40–52. https://doi.org/10.1016/j.envsoft.2013.07.009.

Cosenza, A., Mannina, G., Vanrolleghem, P.A., Neumann, M.C., 2014. Variance-based sensitivity analysis for wastewater treatment plant modeling. Sci. Total Environ. 470–471, 1068–1077. https://doi.org/10.1016/j.scitotenv.2013.10.069.

Fall, C., Espinosa-Rodriguez, A., Flores-Alamo, N., van Loosdrecht, M.C.M., Hooijmans, M.C., 2011. Stepwise calibration of the activated sludge model No. 1 at a partially denitrifying large wastewater treatment plant. Water Environ. Res. 83, 2036–2048. https://doi.org/10.1002/j.1554-7531.2011.tb00270.x.

Flores-Alsina, X., Corominas, L., Neumann, M.B., Vanrolleghem, P.A., 2012. Assessing the use of activated sludge process design guidelines in wastewater treatment plant projects: a methodology based on global sensitivity analysis. Environ. Model. Software 38, 50–58. https://doi.org/10.1016/j.envsoft.2012.04.005.

Flores-Alsina, X. Ardelli, Amerlinck, M., Corominase, Y., Gernaey, L., Guo, K.V., Lindbloma, I., Nopens, E., Porro, I., Shaw, J., A Snip, L., Peter, A., Vanrolleghem, P. A., Jeppsson, U., 2014. Balancing effluent quality, economic cost and greenhouse gas emissions during the evaluation of (plant-wide) control/operational strategies in WWTPs. Sci. Total Environ. 466–467, 616–624. https://doi.org/10.1016/j.scitotenv.2013.07.046.

Freni, G., Mannina, G., Viviani, G., 2009. Urban runoff modelling uncertainty: comparison among Bayesian and pseudo-Bayesian methods. Environ. Model. Software 24, 1100–1111. https://doi.org/10.1016/j.envsoft.2009.03.003.

Friedman, J.H., Roosen, C.B., 1995. An introduction to multivariate adaptive regression splines. Stat. Methods Med. Res. 4, 197–217. https://doi.org/10.1177/096228029500400303.

Gu, Y., Li, Y., Li, X., Luo, P., Wang, H., Wang, X., Wu, J., Li, F., 2017. Energy self-sufficient wastewater treatment plants: feasibilities and challenges. Energy Proc. 105, 3741–3751. https://doi.org/10.1016/j.egypro.2017.03.868.

Henriques, J., Catarino, J., 2017. Sustainable value - an energy efficiency indicator in wastewater treatment plants. J. Clean. Prod. 142, 323. https://doi.org/10.1016/j.jclepro.2016.03.173.

Henze, M., Gujer, W., Mino, T., van Loosedrecht, M.C.M., 2000. Activated Sludge Models ASM1, ASM2, ASM2d and ASM3. IWA Publ., London.

Huang, F., Shen, W., Zhang, X., Seferlis, P., 2020. Impacts of dissolved oxygen control on different greenhouse gas emission sources in wastewater treatment process. J. Clean. Prod. 274, 1–11. https://doi.org/10.1016/j.jclepro.2020.123233.

Hvala, N., Vrecko, D., Bordon, C., 2018. Plant-wide modelling for assessment and optimization of upgraded full-scale wastewater treatment plant performance. Water Pract. Technol. 13 (3), 566–582. https://doi.org/10.2166/wpt.2018.070.

Lindblom, E., Jeppsson, U., Sin, G., 2020. Identification of behavioural model input data sets for WWTP uncertainty analysis. Water Sci. Technol. 81, 1558–1568. https://doi.org/10.2166/wst.2019.427.

Mannina, G., Cosenza, A., Vanrolleghem, P.A., Viviani, G., 2011a. A practical protocol for calibration of nutrient removal wastewater treatment models. J. Hydroinf. 13, 575–595. https://doi.org/10.2166/hydro.2011.041.

Mannina, G., Di Bella, G., Viviani, G., 2011b. An integrated model for biological and physical process simulation in membrane bioreactors (MBR). J. Membr. Sci. 376, 56–69. https://doi.org/10.1016/j.memsci.2011.04.003.

Mannina, G., Cosenza, A., Viviani, G., 2016. Sensitivity and uncertainty analysis of an integrated membrane bioreactor model. Desalination Water Treat. 57, 9531–9548. https://doi.org/10.1080/19443994.2015.1030780.

Mąkinia, J., Rosenwinkel, K.H., Swiniarski, M., Dobiegala, M., 2006. Experimental and model-based evaluation of the role of denitrifying polyphosphate accumulating organisms at two large scale WWTPs in northern Poland. Water Sci. Technol. 54, 73–81. https://doi.org/10.2166/wst.2006. 711.

Mąkinia, J., Zaborowska, E., 2020. Mathematical Modelling and Computer Simulation of Activated Sludge Systems, second ed. IWA Publishing, London.

Mąkinia, J., Rosewinkel, K., Spering, V., 2005. Long-term simulation of the activated sludge process at the Hanover-Gümmerwald pilot WWTP. Water Res. 39, 1489–1502. https://doi.org/10.1016/j.watres.2005.01.023.

Petersen, B., Gernaey, K., Henze, M., Vanrolleghem, P.A., 2002. Evaluation of an ASM1 model calibration procedure on a municipal – industrial wastewater treatment plant. J. Hydroinf. 4, 15–38. https://doi.org/10.2166/hydro.2002.0003.

Pocquet, M., Wu, Z., Queinnec, I., Spérandio, M., 2016. A two pathway model for N2O emissions by ammonium oxidizing bacteria supported by the NO/N2O variation. Water Res. 88, 948–959. https://doi.org/10.1016/j.watres.2015.11.029.

Romanowicz, J., Beven, K., 2006. Comments on generalized likelihood uncertainty estimation. Reliab. Eng. Syst. Saf. 91, 1315–1321. https://doi.org/10.1016/j.ress.2005.11.030.

Sathyamoorthy, S., M Vogel, R.M., Chapra, S.C., Ramsburg, A.C., 2014. Uncertainty and sensitivity analyses using GLUE when modeling inhibition and pharmaceutical cometabolism during nitrification. Environ. Model. Software 60, 219–227. https://doi.org/10.1016/j.envsoft.2014.06.006.

Shahsavania, D., Tarantolab, S., Ratto, M., 2010. Evaluation of MARS modeling technique for sensitivity analysis of model output. Procedia Social and Behavioral Sciences 2, 7737–7738. https://doi.org/10.1016/j.sbspro.2010.05.204.

Sin, G., Gernaey, K.V., Neumann, M.B., van Loosdrecht, M.C., Gujer, W., 2011. Global sensitivity analysis in wastewater treatment plant model applications: prioritizing sources of uncertainty. Water Res. 45, 639–651. https://doi.org/10.1016/j.watres.2010.08.025.

Swinarski, M., Mąkinia, J., Stensel, H.D., Czerwionka, K., Drewnowski, J., 2012. Modeling external carbon addition in biological nutrient removal processes with an extension of the International Water Association activated sludge model. Water Environ. Res. 84, 646–655. https://doi.org/10.2175/106143012x13373550426670.

Takács, I., Patry, G., Nolasco, D., 1991. A dynamic model of the clarification-thickening process. Water Res. 25, 1263–1271. https://doi.org/10.1016/0043-1354(91)90066-Y.

Wang, X., Kvaal, K., Ratnaweera, H., 2019. Explicit and interpretable nonlinear soft sensor models for influent surveillance at a full-scale wastewater treatment plant. J. Process Control 77, 1–6. https://doi.org/10.1016/j.jprocont.2019.03.005.

Wu, X., Yang, Y., Wu, G., Mao, J., Zhou, T., 2016. Simulation and optimization of a coking wastewater biological treatment process by activated sludge models (ASM). J. Environ. Manag. 165, 235–242. https://doi.org/10.1016/j.jenvman.2015.09.041.

Zaborowska, E., Czerwionka, K., Mąkinia, J., 2017. Strategies for achieving energy neutrality in biological nutrient removal systems – a case study of the Slupsk WWTP (northern Poland). Water Sci. Technol. 75, 727–740. https://doi.org/10.2166/wst.2016.564.

Zaborowska, E., Lu, X., Mąkinia, J., 2019. Strategies for mitigating nitrous oxide production and decreasing the carbon footprint of a full-scale combined nitrogen and phosphorus removal activated sludge system. Water Res. 162, 53–63. https://doi.org/10.1016/j.watres.2019.06.057.

Zhao, G., Garrido – Baserba, M., Reifsnyder, S., Xu, J.C., Ross, D., 2019. Comparative energy and carbon footprint analysis of biosolids management strategies in water resource recovery facilities. Sci. Total Environ. 665, 762–773. https://doi.org/10.1016/j.scitotenv.2019.02.024.

Zhu, A., Guo, J., Ni, B.J., Wang, S., Yang, Q., Peng, Y., 2015. A novel protocol for model calibration in biological wastewater treatment. Sci. Rep. 5, 8493. https://doi.org/10.1038/srep08493.

Zonta, Ž.J., Flotats, X., Magrí, A., 2014. Estimation of parameter uncertainty for an activated sludge model using Bayesian inference: a comparison with the frequentist method. Environ. Technol. 35, 1618–1629. https://doi.org/10.1080/09593330.2013.876450.